

DATA-INDEPENDENT MODULE-AWARE PRUNING FOR HIERARCHICAL VISION TRANSFORMERS

Yang He, Joey Tianyi Zhou*

CFAR, Agency for Science, Technology and Research, Singapore

IHPC, Agency for Science, Technology and Research, Singapore

{He_Yang, Joey_Zhou}@cfar.a-star.edu.sg

ABSTRACT

Hierarchical vision transformers (ViTs) have two advantages over conventional ViTs. First, hierarchical ViTs achieve linear computational complexity with respect to image size by local self-attention. Second, hierarchical ViTs create hierarchical feature maps by merging image patches in deeper layers for dense prediction. However, existing pruning methods ignore the unique properties of hierarchical ViTs and use the magnitude value as the weight importance. This approach leads to two main drawbacks. First, the “local” attention weights are compared at a “global” level, which may cause some “locally” important weights to be pruned due to their relatively small magnitude “globally”. The second issue with magnitude pruning is that it fails to consider the distinct weight distributions of the network, which are essential for extracting coarse to fine-grained features at various hierarchical levels.

To solve the aforementioned issues, we have developed a Data-independent Module-Aware Pruning method (DIMAP) to compress hierarchical ViTs. To ensure that “local” attention weights at different hierarchical levels are compared fairly in terms of their contribution, we treat them as a **module** and examine their contribution by analyzing their information distortion. Furthermore, we introduce a novel weight metric that is solely based on weights and does not require input images, thereby eliminating the **dependence** on the patch merging process. Our method validates its usefulness and strengths on Swin Transformers of different sizes on ImageNet-1k classification. Notably, the top-5 accuracy drop is only 0.07% when we remove 52.5% FLOPs and 52.7% parameters of Swin-B. When we reduce 33.2% FLOPs and 33.2% parameters of Swin-S, we can even achieve a 0.8% higher relative top-5 accuracy than the original model. Code is available at: <https://github.com/he-y/Data-independent-Module-Aware-Pruning>.

1 INTRODUCTION

Vision transformers Dosovitskiy et al. (2020); Touvron et al. (2020); Yuan et al. (2021) have achieved state-of-the-art (SOTA) performance in the area of computer vision, including image classification, detection, and segmentation. However, the utilization of self-attention and the removal of the convolutions cause vision transformers Dosovitskiy et al. (2020); Liu et al. (2021) heavy computational burdens and significant parameter counts. Therefore, it is necessary to trim the model to reduce the computational cost and required storage.

It is challenging to apply conventional CNN weight pruning methods directly to Vision Transformers since they have different structures and weight properties Raghu et al. (2021); Park & Kim (2022). The most important structure of modern CNNs such as VGGNet Simonyan & Zisserman (2015) and ResNet He et al. (2016) are convolutional layers. As shown in Figure 1, the convolutional layers of ResNet-50 contribute to 92.0% parameters and 99.9% floating-point operations (FLOPs) of the whole network. In contrast, convolutional layers merely contribute 0.1% to parameters and 0.1% to FLOPs in the Swin Transformer. The special structure of ViTs should thus be considered during the pruning process.

*Corresponding Author

Although there have been attempts to prune conventional ViTs, the unique characteristics of hierarchical ViTs are not fully explored. Local attention is a fundamental feature of hierarchical ViTs, requiring attention computation within a window rather than over the entire image. While this reduces computation on a large scale, it also poses a question: attention weights within one window cannot be compared with those of another window, even if both windows belong to the same image.

We use an example to explain the problem of the previous magnitude pruning methods. Assume the attention value of window A ranges from 0 to 0.3, and that of window B ranges from 0 to 0.7. Previous magnitude pruning methods Han et al. (2015b) will make this pruning decision: before removing the weights larger than 0.3 in window B , all the weights in window A should be removed. However, this decision may not always be correct as pruning all weights in a particular window, such as window A , could lead to the loss of an important object in the image. Therefore, when determining the least important attention weight in an image, we should not take magnitude into account, but rather rank them based on their contribution.

The second characteristic of hierarchical ViTs is that image patches are merged at higher hierarchical scales. In contrast, conventional ViTs Dosovitskiy et al. (2020); Touvron et al. (2020) have the same number of image patches at different levels. The patch merging characteristic of hierarchical ViTs is designed to extract features ranging from coarse to fine-grained for dense prediction. To achieve this property, the weight distribution of different layers should adapt to the image patches at those layers. To minimize the impact of varying image patch sizes, the weight importance metric should be data-independent. Using the magnitude value as a weight metric is the easiest way to ensure data independence. However, it is not valid when comparing attention values across windows or weight values across layers.

In the paper, we propose a Data-independent Module-Aware Pruning method (DIMAP) to address the above two problems together. First, we include different layers within a module and evaluate weight importance at the level of **module** rather than window or layer. By analyzing the Frobenius distortion Park et al. (2020) incurred by a single weight, we can obtain their weight importance and safely compare the contribution of all weights. This allows us to evaluate the importance of weights within a module, regardless of their location within the windows or layers. Further, we analyze the information distortion at the module level and develop a novel data-independent weight importance metric. The proposed data-independent module-aware weight importance metric in DIMAP has several desirable properties. Firstly, it provides a “global” ranking of the importance of weights at the module level without altering the “local” ranking within a layer, making it a generalization method for layer-wise magnitude pruning. Secondly, it does not use any extra parameters and is purely based on weight values, making it simple and efficient. Finally, it can be applied without the need for complex pruning sensitivity analysis, allowing for efficient one-shot pruning.

Contributions are summarized as follows: (1) We analyze the Frobenius distortion incurred by single-weight and module-level pruning. (2) We propose a data-independent weight importance metric to address the issues of previous pruning methods. (3) Experiments validate that our results are comparable to the state-of-the-art results on image classification benchmarks.

2 RELATED WORKS

CNNs Pruning. **1) Weight Pruning.** Weight pruning LeCun et al. (1990); Han et al. (2015b;a) aims to prune the fine-grained weights of the network. For example, Han et al. (2015b) proposes to remove the small weights whose absolute values are below the threshold. Guo et al. (2016) proposes to discard weights dynamically during the training process. Lebedev & Lempitsky (2016) utilizes the group-sparsity regularization on the loss function to shrink some entire groups of weights toward

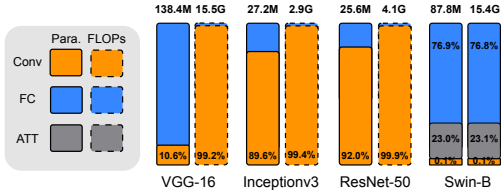


Figure 1: Parameters and FLOPs for different components of CNNs (VGG-16, Inceptionv3, ResNet-50) and Swin Transformer. “Conv” = Convolutional layers, “FC” = Fully-connected layers, “ATT” = Attention layers. The numbers on top of the histograms are the total parameters and FLOPs of the network. The percentage numbers listed inside histograms are the contribution from the corresponding layers. Note that norm layers and down-sampling layers are not included for better visualization.

zeros. However, these weight pruning methods are designed for CNNs, so it is difficult to directly apply these methods to vision transformers with different properties Raghu et al. (2021); Park & Kim (2022). **2) Filter Pruning.** Filter pruning Li et al. (2017); He et al. (2017); Luo et al. (2017); He et al. (2018a; 2019); Suau et al. (2018); He & Xiao (2023) removes the filters entirely to obtain models with structured sparsity, so the pruned convolutional models can achieve better acceleration. Li et al. (2017) uses L1-norm to evaluate the importance of filters of the network. He et al. (2018b) leverages reinforcement learning to find the redundancy for each layer automatically. However, there are not so many “filters” in vision transformers, so we are not able to utilize these algorithms.

Variants of Vision Transformer. Vision transformer is firstly proposed in ViT Dosovitskiy et al. (2020), which utilizes attention not on pixels but instead on small patches of the images. After this, different variants of vision transformers Srinivas et al. (2021); Yuan et al. (2021); Wang et al. (2021); Chen et al. (2021a); Chu et al. (2021b); Han et al. (2021); Xu et al. (2021); Jiang et al. (2021); Xia et al. (2022); Mangalam et al. (2022); Gong et al. (2022); Li et al. (2022b); Mehta & Rastegari (2022); Song et al. (2022); Shao et al. (2022); Tang et al. (2022a;b); Yang et al. (2022a) are emerging. DeiT Touvron et al. (2020) introduces a distillation token to make the student network learns from the teacher network through attention. BoTNet Srinivas et al. (2021) proposes to replace the spatial convolutions with global self-attention in the final three bottleneck blocks of a ResNet. T2T-ViT Yuan et al. (2021) introduces a layer-wise Tokens-To-Token transformation to train the vision transformer from scratch. PVT Wang et al. (2021) utilizes a pyramid structure for dense prediction tasks. CrossViT Chen et al. (2021a) learns multi-scale feature representations with ViT. TNT Han et al. (2021) introduces Transformer in Transformer for excavating features of objects in different scales and locations. CoaT Xu et al. (2021) empowers image transformers with enriched multi-scale and contextual modeling capabilities. LV-ViT Jiang et al. (2021) proposes a new training loss for ViT by taking advantage of all the patch tokens. Swin Transformer Liu et al. (2021) attracts attention for its hierarchical structure and efficient shift window attention.

Vision Transformer Compression. Some parallel methods Heo et al. (2021); Graham et al. (2021); Pan et al. (2021); Yue et al. (2021); Shu et al. (2021); Chu et al. (2021a); Yang et al. (2021b); Liang et al. (2022); Yin et al. (2022); Zhang et al. (2022a); Yang et al. (2022b); Li et al. (2022a); Chen et al. (2022b); Zhang et al. (2022b); Yu et al. (2022); Yu & Xiang (2023); Yang et al. (2023); Chuanyang et al. (2022) are proposed for vision transformer compression and acceleration. **1)** This direction focuses on the redundancy of networks, and the structures of the original network are mostly kept. An important direction is to reduce the **input image tokens** Lee et al. (2023). For example, DynamicViT Rao et al. (2021) prunes redundant tokens progressively. EViT Liang et al. (2022) reorganizes the token to reduce the computational cost of multi-head self-attention. SViTE Chen et al. (2021c) proposes a sparse ViT with a trained token selector. **2)** Another direction is to handle the **network itself**. VTP Zhu et al. (2021) prunes the unimportant features of the ViT with sparsity regularization. AutoFormer Chen et al. (2021b) uses an architecture search framework for vision transformer search. As-ViT Chen et al. (2022c) automatically scales up ViTs. UVC Yu et al. (2021) assembles three effective techniques, including pruning, layer skipping, and knowledge distillation, for efficient ViT. NViT Yang et al. (2021a) uses structural pruning with latency-aware regularization on all parameters of the vision transformer. Most previous compression literature Chen et al. (2021c); Zhu et al. (2021); Chen et al. (2022c; 2021b) focus on pruning conventional ViTs such as DeiT Touvron et al. (2020), which use global self-attention. In contrast, hierarchical ViTs such as Swin Transformer utilize local self-attention to save computational costs. Therefore, it is more difficult to compress hierarchical ViTs than conventional ViTs.

3 MODULE-AWARE PRUNING

3.1 PRELIMINARIES

Assuming a Swin Transformer has L layers, and $\mathbf{W}^{(l)} \in \mathbb{R}^{K \times K \times N_I^{(l)} \times N_O^{(l)}}$ is the weight for the l_{th} layer, where K is the kernel size, $N_I^{(l)}$ and $N_O^{(l)}$ is the number of input and output channels, respectively. The first layer of the Swin Transformer is the patch-embedding layer. It is a convolutional layer, so $K > 1$ and the dimension of this patch-embedding layer is 4. For the latter attention-related layers and fully-connected layers, the dimension of these layers is 2, so we can view the value of K as $K = 1$. LayerNorm (LN) layers are 1-dimension vectors, and these layers only contribute a small portion of FLOPs and storage.



Figure 2: Weight distributions for different functional layers for the first and second Swin Transformer block. The meaning of QKV, PRJ, FC1 and FC2 can be found in Figure 3. The x-axis indicates the values of the weights, and the y-axis denotes the ratios of weights.

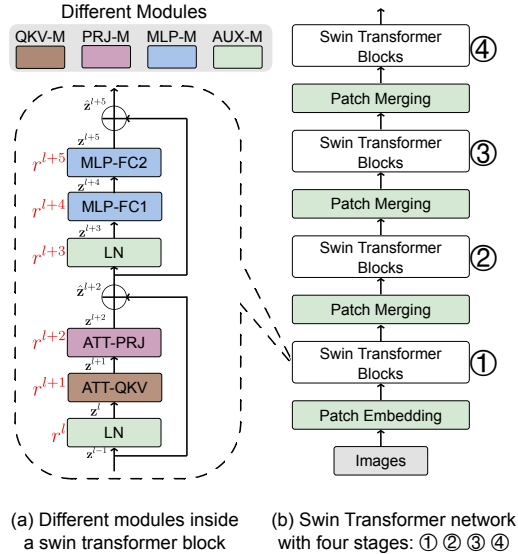


Figure 3: Categorize network layers to different modules regarding (a) Swin Transformer block; (b) Swin Transformer network. The left figure contains detailed layers of a Swin Transformer block. There are four stages in Swin Transformer. Different colors represent different modules, including the attention-related module (QKV-M and PRJ-M), the multilayer perceptron-related module (MLP-M), and the auxiliary module (AUX-M).

Weight Distributions. The weight distributions for different functional layers are shown in Figure 2. The first observation is a notable difference in the weight distribution of the QKV layer between the first and second blocks: the QKV layer of the first block contains a significantly higher number of zeros than that of the second block. The dissimilarity in the distributions supports our statement that a direct comparison of attention with their magnitude is not appropriate. Moreover, even with the same block, different functional layers have various distributions. Applying a magnitude pruning threshold of 0.03 would lead to the removal of approximately 30% of the weights from the QKV and PRJ layers, but up to 80% of the weights from the FC1 and FC2 layers. It is clear that magnitude pruning results in unbalanced pruning outcomes for these layers. To ensure a fair comparison of weights across different layers, we employ the information distortion analysis as the weight metric for pruning, as shown in Sec. 3.2.

Module Definition The definition of modules is shown in Figure 3. More details can be found in Appendix B.

3.2 DISTORTION ANALYSIS AND WEIGHT METRIC

Single Layer Analysis. We first utilize a single fully-connected layer ¹ to consider the pruning problem from the perspective of minimizing ℓ_2 distortion after pruning Neyshabur et al. (2015); Lee et al. (2020). Supposing an input $x \in \mathbb{R}^n$ and a weight tensor $W \in \mathbb{R}^{m \times n}$, the pruning operation can be viewed as $\bar{W} := M \odot W$, where M is a binary mask whose entries are either 0 or 1. s is the sparsity constraint $\|M\|_0 \leq s$. We aim to find a pruning mask M to minimize the difference between the output from a pruned and an unpruned layer:

$$\min_{\|M\|_0 \leq s} \sup_{\|x\|_2 \leq 1} \|Wx - (M \odot W)x\|_2 \tag{1}$$

¹Attention layers include similar matrix multiplications for Q, K and V.

where $\|x\|_2 \leq 1$ is supported on the unit ball. Then the ℓ_2 distortion can be bounded as:

$$\|Wx - (M \odot W)x\|_2 \leq \|W - M \odot W\|_2 \cdot \|x\|_2 \quad (2)$$

Therefore, solving Equation 1 is equivalent to solving:

$$\min_{\|M\|_0 \leq s} \|W - M \odot W\| \quad (3)$$

where $\|\cdot\|$ denotes the spectral norm $\|W\| = \sup_{\xi \neq 0} \frac{\|W\xi\|_2}{\|\xi\|_2}$. With Cauchy-Schwarz inequality, the operation can be relaxed to Frobenius distortion minimization:

$$\min_{\|M\|_0 \leq s} \|W - M \odot W\|_F \quad (4)$$

Module Level Analysis. Suppose the output of a network $W^{(1:L)} = (W^{(1)}, \dots, W^{(L)})$ given the input x is:

$$f(x; W^{(1:L)}) = W^{(L)} \sigma(\dots W^{(2)} \sigma(W^{(1)} x) \dots) \quad (5)$$

As shown in the previous section, a module consists of multiple layers. Suppose $P = \{l_1, l_2, \dots, l_n\}$ is the set that includes all the layers in the module. Pruning a module aims to minimize the following:

$$\min_{\substack{i \in P \\ \|M^{(i)}\|_0 \leq s}} \sup_{\|x\|_2 \leq 1} \left\| f(x; W^{(1:L)}) - f(x; \widetilde{W}^{(1:L)}) \right\|_2 \quad (6)$$

where $\widetilde{W}^{(1:L)}$ is the network after pruning a module. Since directly solving Equation 6 is difficult, we approximate the distortion in Equation 6 by pruning a single connection. Assume $\widetilde{W}^{(l)} := M^{(l)} \odot W^{(l)}$ indicates the l_{th} weight layer after pruning and $l \in \{l_1, l_2, \dots, l_n\}$. In this situation, we have an upper bound²:

$$\begin{aligned} & \sup_{\|x\|_2 \leq 1} \left\| f(x; W^{(1:L)}) - f(x; W^{(1:l-1)}, \widetilde{W}^{(l)}, W^{(l+1:L)}) \right\|_2 \\ & \leq \left\| W^{(l)} - \widetilde{W}^{(l)} \right\|_F \cdot \prod_{\substack{j \neq l \\ j \in [1, L]}} \left\| W^{(j)} \right\|_F \end{aligned} \quad (7)$$

Weight Metric. With the above analysis of distortion minimization, the last step is to convert the above weight selection process to a data-independent weight importance metric. To rank weights inside a module, we rewrite the right side of the Equation 7 as:

$$\frac{\left\| W^{(l)} - \widetilde{W}^{(l)} \right\|_F}{\left\| W^{(l)} \right\|_F} \cdot \prod_{j \in [1, L]} \left\| W^{(j)} \right\|_F \quad (8)$$

In this formulation, the right side of Equation 8 has no influence on pruning since $\widetilde{W}^{(l)}$ is not included in the product term $\prod_{j=1}^L \left\| W^{(j)} \right\|_F$. Then the distortion of pruning can be evaluated with the left side (the algebraic fraction) of Equation 8. We look into the numerator of the fraction:

$$\left\| W^{(l)} - \widetilde{W}^{(l)} \right\|_F = \sqrt{\sum_{\substack{i \in \{1, \dots, m\} \\ j \in \{1, \dots, n\}}} (1 - M_{ij}) W_{ij}^2} \quad (9)$$

where i and j is the index of W and M . To minimize Equation 9, for the top largest W_{ij}^2 , $(1 - M_{ij})$ should be 0.

We sort the weights of $W^{(l)}$ in descending order and get $\{W_{p_1}, W_{p_2}, \dots, W_{p_m \times n}\}$, where W_{p_1} is the largest weight. In the step of removing W_{p_j} , the current $W^{(l)}$ consists of $\{W_{p_1}, W_{p_2}, \dots, W_{p_j}\}$

²Please see proof in Supplementary.

since weights smaller than W_{p_j} are already pruned. After pruning W_{p_j} , the current $\widetilde{W}^{(l)}$ consists of $\{W_{p_1}, W_{p_2}, \dots, W_{p_{j-1}}\}$. Then we can rewrite the left side of Equation 8 to get the weight importance to minimize the distortion:

$$\text{Imp}(W_{p_j}) := \frac{(W_{p_j})^2}{\sum_{i \leq p_j} (W_i)^2} \quad (10)$$

The proposed weight importance has several advantages. 1) This is data-independent and does not require extra parameters other than the weight values. 2) We can conduct one-shot pruning to save computational costs.

4 EXPERIMENTS

4.1 EXPERIMENTAL SETTING

Dataset and Architecture. We follow previous works Chen et al. (2021c); Yu et al. (2021); Chen et al. (2021b) by validating our method on the ImageNet-1K Russakovsky et al. (2015) benchmark dataset. ImageNet-1K contains 1.28 million training images and 50k validation images of 1,000 classes. In our experiments, the input resolution is 224×224 . The architectures include Swin-T, Swin-S and Swin-B. Note that the numbers of Swin Transformer are cited from the authors’ official Github repository³. These numbers are slightly different from those reported in their paper Liu et al. (2021): 0.19% higher for Swin-S, 0.14% lower for Swin-T.

Network Training. We utilize the same training schedules as Liu et al. (2021) when training. Specifically, we employ an AdamW optimizer for 300 epochs using a cosine decay learning rate scheduler and 20 epochs of linear warm-up. The initial learning rate is 0.001, the weight decay is 0.05, and the batch size is 1024. Our data augmentation strategies are also the same as those of Liu et al. (2021) and include color jitter, AutoAugment Cubuk et al. (2018), random erasing Zhong et al. (2020), mixup Zhang et al. (2017), and CutMix Yun et al. (2019).

Pruning Setting. We utilize different pruning ratios to analyze the accuracies for models with different sizes. For the fine-tuning process, we use AdamW optimizer for 30 epochs using a cosine decay learning rate scheduler Loshchilov & Hutter (2017). The base learning rate is $2e-5$, and the minimum learning rate is $2e-7$. The number of warm-up epochs is 15, and the final learning rate of the linear warm-up process is $2e-8$. The weight decay is $1e-8$. During pruning, we keep the AUX-M and prune the other three modules.

We follow UVC Yu et al. (2021) in utilizing FLOPs for acceleration measurements and use the number of non-zero parameters to measure the required storage Han et al. (2015b). We compare with state-of-the-art image classifiers variants including ViT Dosovitskiy et al. (2020), DeiT Touvron et al. (2020), BoTNet Srinivas et al. (2021), T2T-ViT Yuan et al. (2021), PVT Wang et al. (2021), CrossViT Chen et al. (2021a), CPVT Chu et al. (2021b), TNT Han et al. (2021), TransMix Chen et al. (2022a), MobileViTv2 Mehta & Rastegari (2023), STViT Chang et al. (2023), Slide-Swin-T Pan et al. (2023) Flatten-Swin-T Han et al. (2023) Long et al. DeiT-S Long et al. (2023) and vision transformer acceleration methods including VTP Zhu et al. (2021), UVC Yu et al. (2021), SViTE Chen et al. (2021c), AutoFormer Chen et al. (2021b), As-ViT Chen et al. (2022c), and AdaViT Chen et al. (2022d), A-ViT Yin et al. (2022), ViT-Slim Chavan et al. (2022), WDPruning Yu et al. (2022), NViT-S Yang et al. (2023), X-Pruner Yu & Xiang (2023). For all of these comparisons, results with the nearest parameters and FLOPs with our methods are listed for a better comparison.

4.2 PRUNING SWIN TRANSFORMER

The results of pruning Swin Transformers are shown in Table 1. For every network, we set three target FLOPs reduction ratios, naming them DIMAP1, DIMAP2, DIMAP3. For pruning Swin-B, when we remove 14.3% parameters and 14.4% FLOPs, we can improve top-1 accuracy by 0.04%. This result indicates that pruning Swin Transformer has a similar regularization effect as pruning CNNs.

³<https://github.com/microsoft/Swin-Transformer>

Method	Top-1 acc.(%)	Top-1 acc.↓ (%)	Top-5 acc.(%)	Top-5 acc.↓ (%)	Para.	Para. ↓(%)	FLOPs (%)	FLOPs ↓ (%)
Swin-B Liu et al. (2021)	83.48	–	96.46	–	87.8M	–	15.4G	–
Swin-B-DIMAP1	83.52	-0.04	96.43	0.03	75.2M	14.3	13.2G	14.4
Swin-B-DIMAP2	83.43	0.05	96.42	0.04	58.4M	33.4	10.2G	33.5
Swin-B-DIMAP3	83.28	0.20	96.39	0.07	41.7M	52.5	7.3G	52.7
Swin-S Liu et al. (2021)	83.19	–	96.23	–	49.6M	–	8.7G	–
Swin-S-DIMAP1	83.08	0.11	96.25	-0.02	42.5M	14.2	7.5G	14.3
Swin-S-DIMAP2	82.99	0.20	96.26	-0.03	33.1M	33.2	5.8G	33.2
Swin-S-DIMAP3	82.63	0.56	96.12	0.11	23.7M	52.2	4.1G	52.3
Swin-T Liu et al. (2021)	81.16	–	95.48	–	28.3M	–	4.5G	–
Swin-T-DIMAP1	81.17	-0.01	95.47	0.01	24.4M	13.7	3.8G	13.9
Swin-T-DIMAP2	81.11	0.05	95.42	0.06	19.2M	32.0	3.0G	32.4
Swin-T-DIMAP3	80.35	0.81	95.22	0.26	14.0M	50.3	2.2G	50.8

Table 1: Comparison of the pruned Swin Transformer on ImageNet-1K. The “acc. ↓” is the accuracy drop between pruned model and the baseline model (smaller values are better). The negative value of “acc. ↓” means the performance of the pruned model is better than the original model. “Para. ↓” and “FLOPs ↓” are the ratio of removed parameters and FLOPs, respectively.

When pruning about 33.2% of the FLOPs in Swin-S, the top-5 accuracy improves by 0.03%. Although Swin-T is the smallest Swin Transformer model, we can still achieve superior performance. When we remove 13.7% FLOPs or 13.9% FLOPs, the top-1 accuracy drop improves by 0.01%. If we further increase the pruning ratio to 50.8% FLOPs, the top-5 accuracy drop is 0.26%. These results demonstrate that DIMAP works well on variants of the Swin Transformer.

Comparing the “large pruned” to the “small unpruned” model is interesting. We find our pruned models achieve better accuracies with fewer parameters. For example, when we compare Swin-B-DIMAP3 (“large pruned”) and Swin-S (“small unpruned”), our Swin-B-DIMAP3 model achieves 0.09% higher accuracy with 7.9M fewer parameters. Similarly, if we look further at Swin-S-DIMAP3 (“large pruned”) and Swin-T (“small unpruned”), we find this scenario happens again: our Swin-S-DIMAP3 achieves 0.53% higher accuracy with 4.6M fewer parameters. These results indicate that our DIMAP method effectively shrinks large models into small models and finds models with better accuracy-computation trade-offs than the originally designed models.

4.3 COMPARISON WITH STATE-OF-THE-ART METHODS

Comparison with Vision Transformer Variants (Table 2a). Our Swin-T-DIMAP2, Swin-S-DIMAP1 and Swin-B-DIMAP3 perform better than PVT-Small, PVT-Medium, PVT-Large Wang et al. (2021), respectively. Our Swin-S-DIMAP3 achieves a 0.33% higher top-1 accuracy with 0.5G fewer FLOPs required than Slide-Swin-T Pan et al. (2023). Our Swin-S-DIMAP3 has a similar improvement over Flatten-Swin-T Han et al. (2023). The Flatten Han et al. (2023) and Slide Pan et al. (2023) methods demonstrate a better trade-off on Swin-S and Swin-B architectures as they focus on improving the attention process. Our proposed method focuses on weight and can be combined with their approaches to achieve higher performance. We only report the results of BAT Long et al. (2023) on DeiT since the Swin transformer is not included in the original BAT paper. These results validate the effectiveness of our DIMAP method.

Comparison with Vision Transformer Compression Methods (Table 2b). Our Swin-B-DIMAP3 utilizes 6.3M fewer parameters and 2.7G fewer FLOPs than VTP Zhu et al. (2021) with 2.58% better accuracy. We also achieve 0.7G fewer FLOPs than UVC Yu et al. (2021) with 2.68% higher accuracy. Our Swin-B-DIMAP3 achieves 1.72% better accuracy than SViTE Chen et al. (2021c) with 10.3M fewer parameters and 3.5G fewer FLOPs. Our Swin-S-DIMAP3, Swin-B-DIMAP3, Swin-B-DIMAP1 also performs better than As-ViT-Small Chen et al. (2022c), As-ViT-Base Chen et al. (2022c), As-ViT-Large Chen et al. (2022c), respectively. Compared to X-Pruner Yu & Xiang (2023), our Swin-S-DIMAP2 has 0.99% better accuracy and 0.2G fewer FLOPs. These results demonstrate that our DIMAP achieves a better trade-off between accuracy and computation than existing compression methods.

method	Image size	Para.	FLOPs	ImageNet top-1 acc.	method	image size	#param.	FLOPs	ImageNet top-1 acc.
ViT-B/16 Dosovitskiy et al. (2020)	384 ²	86M	55.4G	77.9	VTP Zhu et al. (2021)	224 ²	48.0M	10.0G	80.7
ViT-L/16 Dosovitskiy et al. (2020)	384 ²	307M	190.7G	76.5	VTP Zhu et al. (2021)	224 ²	67.3M	13.8G	81.3
DeiT-S Touvron et al. (2020)	224 ²	22M	4.6G	79.8	UVC Yu et al. (2021)	224 ²	-	8.0G	80.6
DeiT-B Touvron et al. (2020)	224 ²	86M	17.5G	81.8	SViT-E Chen et al. (2021c)	224 ²	13.3M	2.9G	80.26
DeiT-B Touvron et al. (2020)	384 ²	86M	55.4G	83.1	S ² ViTE Chen et al. (2021c)	224 ²	14.6M	3.1G	79.22
BoT-S1-50 Srinivas et al. (2021)	224 ²	20.8M	4.27G	79.1	SViT-E Chen et al. (2021c)	224 ²	52.0M	10.8G	81.56
T2T-ViT-t-19 Yuan et al. (2021)	224 ²	39.2M	9.8G	82.4	S ² ViTE Chen et al. (2021c)	224 ²	56.8M	11.7G	82.22
T2T-ViT-t-24 Yuan et al. (2021)	224 ²	64.1M	15.0G	82.6	AdaViT Meng et al. (2022)	224 ²	-	3.9G	81.1
PVT-Small Wang et al. (2021)	224 ²	24.5M	3.8G	79.8	ViT-Slim Chavan et al. (2022)	224 ²	17.7M	3.7G	80.6
PVT-Medium Wang et al. (2021)	224 ²	44.2M	6.7G	81.2	AutoFormer Chen et al. (2021b)	224 ²	54M	11G	82.4
PVT-Large Wang et al. (2021)	224 ²	61.4M	9.8G	81.7	A-ViT Yin et al. (2022)	224 ²	22M	3.6G	80.7
CrossViT-18† Chen et al. (2021a)	224 ²	44.3M	9.5G	82.8	WDPruning Yu et al. (2022)	224 ²	-	7.6G	82.41
CPVT-S Chu et al. (2021b)	224 ²	22M	-	79.9	WDPruning Yu et al. (2022)	224 ²	-	6.3G	81.80
CPVT-B Chu et al. (2021b)	224 ²	86M	-	81.9	NViT-S Yang et al. (2023)	224 ²	21M	4.2G	82.19
As-ViT-Small Chen et al. (2022c)	224 ²	29.0M	5.3G	81.2	X-Pruner Yu & Xiang (2023)	224 ²	-	3.2G	80.7
As-ViT-Base Chen et al. (2022c)	224 ²	52.6M	8.9G	82.5	X-Pruner Yu & Xiang (2023)	224 ²	-	6.0G	82.0
As-ViT-Large Chen et al. (2022c)	224 ²	88.1M	22.6G	83.5	Swin-T-DIMAP3	224 ²	14.0M	2.2G	80.35
TNT Han et al. (2021)	224 ²	65.6M	14.1G	82.9	Swin-T-DIMAP2	224 ²	19.2M	3.0G	81.11
TransMix Chen et al. (2022a)	224 ²	86.6M	17.6G	81.8	Swin-T-DIMAP1	224 ²	24.4M	3.8G	81.17
MobileViTv2 Mehta & Rastegari (2023)	224 ²	28.3M	4.5G	81.3	Swin-S-DIMAP3	224 ²	23.7M	4.1G	82.63
STViT-Swin-T Chang et al. (2023)	-	-	3.14G	81.0	Swin-S-DIMAP2	224 ²	33.1M	5.8G	82.99
STViT-Swin-S Chang et al. (2023)	-	-	5.95G	82.8	Swin-S-DIMAP1	224 ²	42.5M	7.5G	83.08
STViT-Swin-B Chang et al. (2023)	-	-	10.48G	83.2	Swin-B-DIMAP3	224 ²	41.7M	7.3G	83.28
Slide-Swin-T Pan et al. (2023)	-	30M	4.6G	82.3	Swin-B-DIMAP2	224 ²	58.4M	10.2G	83.43
Flatten-Swin-T Han et al. (2023)	224 ²	29M	4.5G	82.1	Swin-B-DIMAP1	224 ²	75.2M	13.2G	83.52
BAT-DeiT-S Long et al. (2023)	-	22.1M	3.0G	79.6					

(a) Vision transformer variants.

(b) Vision transformer compression methods.

Table 2: Compare results on ImageNet-1K classification.

Method	Swin-B	Swin-S	Swin-T	Swin-B	Swin-S	Swin-T	Swin-B	Swin-S	Swin-T	Swin-B	Swin-S	Swin-T
Ratio	19%	19%	19%	28%	28%	28%	38%	38%	38%	50%	50%	50%
Uniform	83.25	82.91	80.70	82.27	81.91	79.20	77.73	77.86	72.06	15.26	13.93	6.02
Ours	83.36(+0.11)	82.98(+0.07)	80.87(+0.17)	83.02(+0.75)	82.58(+0.67)	80.24(+1.04)	81.95(+4.22)	81.56(+3.70)	78.54(+4.79)	78.13(+62.87)	76.78(+62.85)	71.36(+65.34)

Table 3: Comparison of uniform magnitude-based pruning with our DIMAP. The ratio here means the proportion of removed parameters after pruning. The numbers in brackets are our top-1 accuracy gain over uniform pruning.

4.4 ADDITIONAL ANALYSIS

Module Pruning Rate Analysis. As shown in Figure 5, we analyze pruning results based on our proposed module-level weight importance. Specifically, we first calculate the module-level weight importance for each module. Then we conduct magnitude pruning to remove the least important weights from the module. Note that a module merely has one threshold for pruning. The pruning thresholds for QKV-M, PRJ-M and MLP-M are 3.8E-7, 4.99E-7 and 1.5E-6, respectively. After pruning, the ratios of the kept parameters for different layers are shown as the y-axis in Figure 5. We have several observations. 1) The lower layers keep a larger ratio of parameters than the higher layers. This phenomenon indicates the higher layers have greater redundancy. 2) In the first and the second Swin Transformer block, we find that the attention-related layers (layer 1,2,5,6) have larger ratios than MLP-related layers (layer 3,4,7,8). This result shows that the attention operation is extremely important for low-level features. 3) We can take a look at Figure 5 and Figure 2 together. Layer 4 and layer 8 in Figure 5 correspond to two FC2 layers in Figure 2. In Figure 5, layer 4 has a smaller weight-kept ratio than layer 8. This pruning result reasonably corresponds to distributions in Figure 2: there are more weights close to zero in layer 4 than in layer 8.

Model	Multiple Modules (%)	Single Module (%)	Difference (%)
Swin-B-DIMAP3	83.28	83.17	0.11
Swin-S-DIMAP3	82.63	82.31	0.32
Swin-T-DIMAP3	80.35	80.12	0.23

Figure 4: Comparison of the theoretical and realistic acceleration. Only the time consumption of the forward procedure is considered.

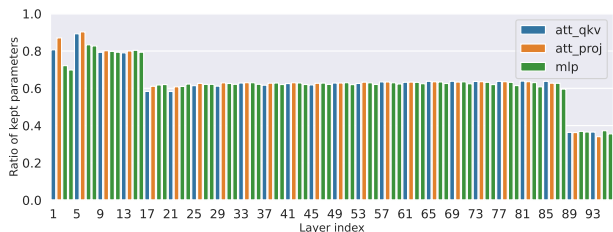


Figure 5: Results of pruning 45% of the parameters from the Swin-S with our module-level weight importance. The x-axis denotes the layer index, and the y-axis indicates the ratio of the remaining parameters. Different colors represent different modules.

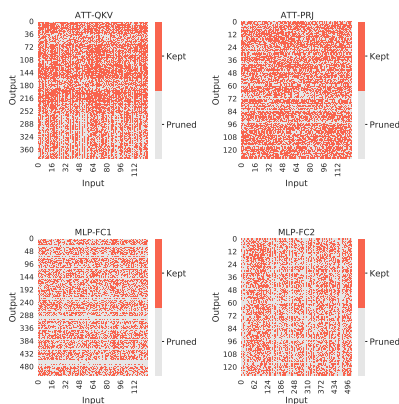


Figure 6: Visualization of four pruned layers in Swin-B. The pruning ratio is 50%. The x-axis is the input dimension, and the y-axis indicates the output dimension. The red areas indicate kept weights, and the grey areas represent pruned weights.

Comparison with Uniform Pruning. In Table 3, we conduct an ablation study by comparing our method to magnitude-based uniform pruning. Apparently, we are better than uniform pruning at all settings. Explicitly, at a small pruning ratio like 19%, our accuracy gain is just about 0.1%. When we increase the pruning ratio to 50%, our DIMAP method achieves a 60+% accuracy gain over uniform pruning. These results validate that the necessity of DIMAP in guaranteeing performance, especially when the pruning ratio is large.

Visualization. We visualize the four DIMAP-pruned layers in the first Swin Transformer block in Figure 6. First, for the figure of ATT-QKV, the y-indexes for “Query, Key, and Value” are [0,127], [128,255], [256,383], respectively. We find the “Query” and “Key” matrix of ATT-QKV is denser than the “Value” matrix. This implies that “Query” and “Key” may suffer more from pruning than “Value”. Second, although ATT-PRJ, MLP-FC1 and MLP-FC2 serve as fully-connected layers, the pattern of ATT-PRJ is quite different from the other two layers. A possible reason is that the input of ATT-PRJ also includes the relative position bias of attention, and ATT-PRJ needs to project this position information. Third, we can even find several rows of weights are removed entirely. For example, in MLP-FC1, no weights are kept when the y-index equals 228 and 231. This phenomenon may further guide us on how to design the size of MLP. Fourth, we find that the pattern of MLP-FC1 is similar to MLP-FC2. This result is another proof that we should categorize MLP-FC1 and MLP-FC2 into the same module.

Model as Module. It is interesting to view the entire model as a single module. In this setting, we keep the auxiliary layers unpruned and view all other layers as a module. This means all the weights are compared based on our novel weight metric. The results shown in Tab. 4 demonstrate our fine-grained module definition in Sec. 3.1 can achieve better performance than “Model as Module”.

5 CONCLUSION AND FUTURE WORK

We introduce DIMAP to compress hierarchical ViTs while considering two key properties of these models. We present two main contributions: an analysis of information distortion at the module level, and a data-independent weight importance metric based on the distortion analysis. A drawback of weight pruning is that it does not bring realistic acceleration on GPUs, and we will explore this direction in the future. Furthermore, we are interested in the performances on downstream tasks such as object detection and segmentation. We are also interested in the performance of our method on other ViT variants.

6 ACKNOWLEDGEMENT

This work was supported in part by A*STAR Career Development Fund (CDF) under C233312004, in part by the National Research Foundation, Singapore, and the Maritime and Port Authority of Singapore / Singapore Maritime Institute under the Maritime Transformation Programme (Maritime AI Research Programme – Grant number SMI-2022-MTP-06).

REFERENCES

- Shuning Chang, Pichao Wang, Ming Lin, Fan Wang, David Junhao Zhang, Rong Jin, and Mike Zheng Shou. Making vision transformers efficient from a token sparsification view. In *Proc. IEEE Conf. Comput. Vis. Pattern Recog.*, pp. 6195–6205, 2023.
- Arnav Chavan, Zhiqiang Shen, Zhuang Liu, Zechun Liu, Kwang-Ting Cheng, and Eric P Xing. Vision transformer slimming: Multi-dimension searching in continuous optimization space. In *Proceedings of the IEEE/CVF Conference on Computer Vision and Pattern Recognition*, pp. 4931–4941, 2022.
- Chun-Fu Richard Chen, Quanfu Fan, and Rameswar Panda. Crossvit: Cross-attention multi-scale vision transformer for image classification. In *Proceedings of the IEEE/CVF International Conference on Computer Vision*, pp. 357–366, 2021a.
- Jie-Neng Chen, Shuyang Sun, Ju He, Philip HS Torr, Alan Yuille, and Song Bai. Transmix: Attend to mix for vision transformers. In *Proceedings of the IEEE/CVF Conference on Computer Vision and Pattern Recognition*, pp. 12135–12144, 2022a.
- Minghao Chen, Houwen Peng, Jianlong Fu, and Haibin Ling. Autoformer: Searching transformers for visual recognition. In *Proceedings of the IEEE/CVF International Conference on Computer Vision*, pp. 12270–12280, 2021b.
- Tianlong Chen, Yu Cheng, Zhe Gan, Lu Yuan, Lei Zhang, and Zhangyang Wang. Chasing sparsity in vision transformers: An end-to-end exploration. *Advances in Neural Information Processing Systems*, 34, 2021c.
- Tianlong Chen, Zhenyu Zhang, Yu Cheng, Ahmed Awadallah, and Zhangyang Wang. The principle of diversity: Training stronger vision transformers calls for reducing all levels of redundancy. In *Proceedings of the IEEE/CVF Conference on Computer Vision and Pattern Recognition*, pp. 12020–12030, 2022b.
- Wuyang Chen, Wei Huang, Xianzhi Du, Xiaodan Song, Zhangyang Wang, and Denny Zhou. Auto-scaling vision transformers without training. In *ICLR*, 2022c.
- Xianing Chen, Qiong Cao, Yujie Zhong, Jing Zhang, Shenghua Gao, and Dacheng Tao. Dearth: Data-efficient early knowledge distillation for vision transformers. In *Proceedings of the IEEE/CVF Conference on Computer Vision and Pattern Recognition*, pp. 12052–12062, 2022d.
- Xiangxiang Chu, Zhi Tian, Yuqing Wang, Bo Zhang, Haibing Ren, Xiaolin Wei, Huaxia Xia, and Chunhua Shen. Twins: Revisiting the design of spatial attention in vision transformers. *Advances in Neural Information Processing Systems*, 34, 2021a.
- Xiangxiang Chu, Zhi Tian, Bo Zhang, Xinlong Wang, Xiaolin Wei, Huaxia Xia, and Chunhua Shen. Conditional positional encodings for vision transformers. *Arxiv preprint 2102.10882*, 2021b. URL <https://arxiv.org/pdf/2102.10882.pdf>.
- Zheng Chuanyang, Zheyang Li, Kai Zhang, Zhi Yang, Wenming Tan, Jun Xiao, Ye Ren, and Shiliang Pu. Savit: Structure-aware vision transformer pruning via collaborative optimization. In *Adv. Neural Inform. Process. Syst.*, 2022.
- Ekin D Cubuk, Barret Zoph, Dandelion Mane, Vijay Vasudevan, and Quoc V Le. Autoaugment: Learning augmentation policies from data. *arXiv preprint arXiv:1805.09501*, 2018.

- Alexey Dosovitskiy, Lucas Beyer, Alexander Kolesnikov, Dirk Weissenborn, Xiaohua Zhai, Thomas Unterthiner, Mostafa Dehghani, Matthias Minderer, Georg Heigold, Sylvain Gelly, et al. An image is worth 16x16 words: Transformers for image recognition at scale. *arXiv preprint arXiv:2010.11929*, 2020.
- Chengyue Gong, Dilin Wang, Meng Li, Xinlei Chen, Zhicheng Yan, Yuandong Tian, Vikas Chandra, et al. Nasvit: Neural architecture search for efficient vision transformers with gradient conflict aware supernet training. In *International Conference on Learning Representations*, 2022.
- Benjamin Graham, Alaaeldin El-Nouby, Hugo Touvron, Pierre Stock, Armand Joulin, Hervé Jégou, and Matthijs Douze. Levit: a vision transformer in convnet’s clothing for faster inference. In *Proceedings of the IEEE/CVF International Conference on Computer Vision*, pp. 12259–12269, 2021.
- Yiwen Guo, Anbang Yao, and Yurong Chen. Dynamic network surgery for efficient DNNs. In *Proc. Adv. Neural Inf. Process. Syst.*, 2016.
- Dongchen Han, Xuran Pan, Yizeng Han, Shiji Song, and Gao Huang. Flatten transformer: Vision transformer using focused linear attention. In *Proc. Int. Conf. Comput. Vis.*, pp. 5961–5971, 2023.
- Kai Han, An Xiao, Enhua Wu, Jianyuan Guo, Chunjing Xu, and Yunhe Wang. Transformer in transformer. In *Adv. Neural Inform. Process. Syst.*, 2021.
- Song Han, Huizi Mao, and William J Dally. Deep compression: Compressing deep neural networks with pruning, trained quantization and huffman coding. In *Proc. Int. Conf. Learn. Represent.*, 2015a.
- Song Han, Jeff Pool, John Tran, and William Dally. Learning both weights and connections for efficient neural network. In *Proc. Adv. Neural Inf. Process. Syst.*, 2015b.
- Kaiming He, Xiangyu Zhang, Shaoqing Ren, and Jian Sun. Deep residual learning for image recognition. In *Proceedings of the IEEE conference on computer vision and pattern recognition*, pp. 770–778, 2016.
- Yang He and Lingao Xiao. Structured pruning for deep convolutional neural networks: A survey. *IEEE Trans. Pattern Anal. Mach. Intell.*, pp. 1–20, 2023. doi: 10.1109/TPAMI.2023.3334614.
- Yang He, Guoliang Kang, Xuanyi Dong, Yanwei Fu, and Yi Yang. Soft filter pruning for accelerating deep convolutional neural networks. In *Proc. Int. Joint Conf. Artif. Intell.*, 2018a.
- Yang He, Ping Liu, Ziwei Wang, and Yi Yang. Pruning filter via geometric median for deep convolutional neural networks acceleration. In *Proc. IEEE Conf. Comput. Vis. Pattern Recognit. (CVPR)*, 2019.
- Yihui He, Xiangyu Zhang, and Jian Sun. Channel pruning for accelerating very deep neural networks. In *Proc. IEEE Int. Conf. Comput. Vis. (ICCV)*, 2017.
- Yihui He, Ji Lin, Zhijian Liu, Hanrui Wang, Li-Jia Li, and Song Han. Amc: Automl for model compression and acceleration on mobile devices. In *Proceedings of the European Conference on Computer Vision (Eur. Conf. Comput. Vis.)*, pp. 784–800, 2018b.
- Byeongho Heo, Sangdoon Yun, Dongyoon Han, Sanghyuk Chun, Junsuk Choe, and Seong Joon Oh. Rethinking spatial dimensions of vision transformers. In *Proceedings of the IEEE/CVF International Conference on Computer Vision*, pp. 11936–11945, 2021.
- Zi-Hang Jiang, Qibin Hou, Li Yuan, Daquan Zhou, Yujun Shi, Xiaojie Jin, Anran Wang, and Jiashi Feng. All tokens matter: Token labeling for training better vision transformers. *Advances in Neural Information Processing Systems*, 34, 2021.
- Vadim Lebedev and Victor Lempitsky. Fast ConvNets using group-wise brain damage. In *Proc. IEEE Conf. Comput. Vis. Pattern Recognit. (CVPR)*, 2016.
- Yann LeCun, John S Denker, and Sara A Solla. Optimal brain damage. In *Proc. Adv. Neural Inf. Process. Syst.*, pp. 598–605, 1990.

- Heejun Lee, Minki Kang, Youngwan Lee, and Sung Ju Hwang. Sparse token transformer with attention back tracking. In *Int. Conf. Learn. Represent.*, 2023.
- Jaeho Lee, Sejun Park, Sangwoo Mo, Sungsoo Ahn, and Jinwoo Shin. Layer-adaptive sparsity for the magnitude-based pruning. *arXiv preprint arXiv:2010.07611*, 2020.
- Changlin Li, Bohan Zhuang, Guangrun Wang, Xiaodan Liang, Xiaojun Chang, and Yi Yang. Automated progressive learning for efficient training of vision transformers. In *Proceedings of the IEEE/CVF Conference on Computer Vision and Pattern Recognition*, pp. 12486–12496, 2022a.
- Hao Li, Asim Kadav, Igor Durdanovic, Hanan Samet, and Hans Peter Graf. Pruning filters for efficient ConvNets. In *Proc. Int. Conf. Learn. Represent.*, 2017.
- Kunchang Li, Yali Wang, Peng Gao, Guanglu Song, Yu Liu, Hongsheng Li, and Yu Qiao. UniFormer: Unified transformer for efficient spatiotemporal representation learning. In *International Conference on Learning Representations*, 2022b.
- Youwei Liang, Chongjian Ge, Zhan Tong, Yibing Song, Jue Wang, and Pengtao Xie. Not all patches are what you need: Expediting vision transformers via token reorganizations. In *International Conference on Learning Representations*, 2022.
- Ze Liu, Yutong Lin, Yue Cao, Han Hu, Yixuan Wei, Zheng Zhang, Stephen Lin, and Baining Guo. Swin transformer: Hierarchical vision transformer using shifted windows. *arXiv preprint arXiv:2103.14030*, 2021.
- Sifan Long, Zhen Zhao, Jimin Pi, Shengsheng Wang, and Jingdong Wang. Beyond attentive tokens: Incorporating token importance and diversity for efficient vision transformers. In *Proc. IEEE Conf. Comput. Vis. Pattern Recog.*, pp. 10334–10343, 2023.
- Ilya Loshchilov and Frank Hutter. SGDR: Stochastic gradient descent with warm restarts. In *Proc. Int. Conf. Learn. Represent.*, 2017.
- Jian-Hao Luo, Jianxin Wu, and Weiyao Lin. ThiNet: A filter level pruning method for deep neural network compression. In *Proc. IEEE Int. Conf. Comput. Vis. (ICCV)*, 2017.
- Karttikeya Mangalam, Haoqi Fan, Yanghao Li, Chao-Yuan Wu, Bo Xiong, Christoph Feichtenhofer, and Jitendra Malik. Reversible vision transformers. In *Proceedings of the IEEE/CVF Conference on Computer Vision and Pattern Recognition*, pp. 10830–10840, 2022.
- Sachin Mehta and Mohammad Rastegari. Mobilevit: light-weight, general-purpose, and mobile-friendly vision transformer. In *International Conference on Learning Representations*, 2022.
- Sachin Mehta and Mohammad Rastegari. Separable self-attention for mobile vision transformers. *Trans. Mach. Learn. Res.*, 2023. ISSN 2835-8856. URL <https://openreview.net/forum?id=tB14yBEjKi>.
- Lingchen Meng, Hengduo Li, Bor-Chun Chen, Shiyi Lan, Zuxuan Wu, Yu-Gang Jiang, and Ser-Nam Lim. Adavit: Adaptive vision transformers for efficient image recognition. In *Proceedings of the IEEE/CVF Conference on Computer Vision and Pattern Recognition*, pp. 12309–12318, 2022.
- Behnam Neyshabur, Ryota Tomioka, and Nathan Srebro. Norm-based capacity control in neural networks. In *Conference on Learning Theory*, pp. 1376–1401. PMLR, 2015.
- Xuran Pan, Tianzhu Ye, Zhuofan Xia, Shiji Song, and Gao Huang. Slide-transformer: Hierarchical vision transformer with local self-attention. In *Proc. IEEE Conf. Comput. Vis. Pattern Recog.*, pp. 2082–2091, 2023.
- Zizheng Pan, Bohan Zhuang, Jing Liu, Haoyu He, and Jianfei Cai. Scalable vision transformers with hierarchical pooling. In *Proceedings of the IEEE/CVF International Conference on Computer Vision*, pp. 377–386, 2021.
- Namuk Park and Songkuk Kim. How do vision transformers work? In *ICLR*, 2022.

- Sejun Park, Jaeho Lee, Sangwoo Mo, and Jinwoo Shin. Lookahead: a far-sighted alternative of magnitude-based pruning. In *Proc. Int. Conf. Learn. Represent.*, 2020.
- Maithra Raghu, Thomas Unterthiner, Simon Kornblith, Chiyuan Zhang, and Alexey Dosovitskiy. Do vision transformers see like convolutional neural networks? *Advances in Neural Information Processing Systems*, 34, 2021.
- Yongming Rao, Wenliang Zhao, Benlin Liu, Jiwen Lu, Jie Zhou, and Cho-Jui Hsieh. Dynamicvit: Efficient vision transformers with dynamic token sparsification. *Advances in neural information processing systems*, 34, 2021.
- Olga Russakovsky, Jia Deng, Hao Su, Jonathan Krause, Sanjeev Satheesh, Sean Ma, Zhiheng Huang, Andrej Karpathy, Aditya Khosla, Michael Bernstein, et al. ImageNet large scale visual recognition challenge. *Int. J. Comput. Vis.*, 2015.
- Wenqi Shao, Yixiao Ge, Zhaoyang Zhang, Xuyuan Xu, Xiaogang Wang, Ying Shan, and Ping Luo. Dynamic token normalization improves vision transformer. In *International Conference on Learning Representations*, 2022.
- Han Shu, Jiahao Wang, Hanting Chen, Lin Li, Yujiu Yang, and Yunhe Wang. Adder attention for vision transformer. *Advances in Neural Information Processing Systems*, 34, 2021.
- Karen Simonyan and Andrew Zisserman. Very deep convolutional networks for large-scale image recognition. In *Proc. Int. Conf. Learn. Represent.*, 2015.
- Hwanjun Song, Deqing Sun, Sanghyuk Chun, Varun Jampani, Dongyoon Han, Byeongho Heo, Wonjae Kim, and Ming-Hsuan Yang. Vidt: An efficient and effective fully transformer-based object detector. In *International Conference on Learning Representations*, 2022.
- Aravind Srinivas, Tsung-Yi Lin, Niki Parmar, Jonathon Shlens, Pieter Abbeel, and Ashish Vaswani. Bottleneck transformers for visual recognition, 2021.
- J Michael Steele. *The Cauchy-Schwarz master class: an introduction to the art of mathematical inequalities*. Cambridge University Press, 2004.
- Xavier Suau, Luca Zappella, Vinay Palakkode, and Nicholas Apostoloff. Principal filter analysis for guided network compression. *arXiv preprint arXiv:1807.10585*, 2018.
- Shitao Tang, Jiahui Zhang, Siyu Zhu, and Ping Tan. Quadtree attention for vision transformers. In *International Conference on Learning Representations*, 2022a.
- Yehui Tang, Kai Han, Yunhe Wang, Chang Xu, Jianyuan Guo, Chao Xu, and Dacheng Tao. Patch slimming for efficient vision transformers. In *Proceedings of the IEEE/CVF Conference on Computer Vision and Pattern Recognition*, pp. 12165–12174, 2022b.
- Hugo Touvron, Matthieu Cord, Matthijs Douze, Francisco Massa, Alexandre Sablayrolles, and Hervé Jégou. Training data-efficient image transformers & distillation through attention. *arXiv preprint arXiv:2012.12877*, 2020.
- Wenhai Wang, Enze Xie, Xiang Li, Deng-Ping Fan, Kaitao Song, Ding Liang, Tong Lu, Ping Luo, and Ling Shao. Pyramid vision transformer: A versatile backbone for dense prediction without convolutions. *arXiv preprint arXiv:2102.12122*, 2021.
- Zhuofan Xia, Xuran Pan, Shiji Song, Li Erran Li, and Gao Huang. Vision transformer with deformable attention. In *Proceedings of the IEEE/CVF Conference on Computer Vision and Pattern Recognition*, pp. 4794–4803, 2022.
- Weijian Xu, Yifan Xu, Tyler Chang, and Zhuowen Tu. Co-scale conv-attentional image transformers. In *Proceedings of the IEEE/CVF International Conference on Computer Vision*, pp. 9981–9990, 2021.
- Chenglin Yang, Yilin Wang, Jianming Zhang, He Zhang, Zijun Wei, Zhe Lin, and Alan Yuille. Lite vision transformer with enhanced self-attention. In *Proceedings of the IEEE/CVF Conference on Computer Vision and Pattern Recognition*, pp. 11998–12008, 2022a.

- Huanrui Yang, Hongxu Yin, Pavlo Molchanov, Hai Li, and Jan Kautz. Nvit: Vision transformer compression and parameter redistribution. *arXiv preprint arXiv:2110.04869*, 2021a.
- Huanrui Yang, Hongxu Yin, Maying Shen, Pavlo Molchanov, Hai Li, and Jan Kautz. Global vision transformer pruning with hessian-aware saliency. In *IEEE Conf. Comput. Vis. Pattern Recog.*, pp. 18547–18557, 2023.
- Jianwei Yang, Chunyuan Li, Pengchuan Zhang, Xiyang Dai, Bin Xiao, Lu Yuan, and Jianfeng Gao. Focal attention for long-range interactions in vision transformers. *Advances in Neural Information Processing Systems*, 34, 2021b.
- Shusheng Yang, Xinggong Wang, Yu Li, Yuxin Fang, Jiemin Fang, Wenyu Liu, Xun Zhao, and Ying Shan. Temporally efficient vision transformer for video instance segmentation. In *Proceedings of the IEEE/CVF Conference on Computer Vision and Pattern Recognition*, pp. 2885–2895, 2022b.
- Hongxu Yin, Arash Vahdat, Jose M Alvarez, Arun Mallya, Jan Kautz, and Pavlo Molchanov. A-vit: Adaptive tokens for efficient vision transformer. In *Proceedings of the IEEE/CVF Conference on Computer Vision and Pattern Recognition*, pp. 10809–10818, 2022.
- Fang Yu, Kun Huang, Meng Wang, Yuan Cheng, Wei Chu, and Li Cui. Width & depth pruning for vision transformers. In *AAAI*, pp. 3143–3151, 2022.
- Lu Yu and Wei Xiang. X-pruner: explainable pruning for vision transformers. In *IEEE Conf. Comput. Vis. Pattern Recog.*, pp. 24355–24363, 2023.
- Shixing Yu, Tianlong Chen, Jiayi Shen, Huan Yuan, Jianchao Tan, Sen Yang, Ji Liu, and Zhangyang Wang. Unified visual transformer compression. In *International Conference on Learning Representations*, 2021.
- Li Yuan, Yunpeng Chen, Tao Wang, Weihao Yu, Yujun Shi, Francis EH Tay, Jiashi Feng, and Shuicheng Yan. Tokens-to-token vit: Training vision transformers from scratch on imagenet. *arXiv preprint arXiv:2101.11986*, 2021.
- Xiaoyu Yue, Shuyang Sun, Zhanghui Kuang, Meng Wei, Philip HS Torr, Wayne Zhang, and Dahua Lin. Vision transformer with progressive sampling. In *Proceedings of the IEEE/CVF International Conference on Computer Vision*, pp. 387–396, 2021.
- Sangdoon Yun, Dongyoon Han, Seong Joon Oh, Sanghyuk Chun, Junsuk Choe, and Youngjoon Yoo. Cutmix: Regularization strategy to train strong classifiers with localizable features. In *Proceedings of the IEEE/CVF international conference on computer vision*, pp. 6023–6032, 2019.
- Hongyi Zhang, Moustapha Cisse, Yann N Dauphin, and David Lopez-Paz. mixup: Beyond empirical risk minimization. *arXiv preprint arXiv:1710.09412*, 2017.
- Jinnian Zhang, Houwen Peng, Kan Wu, Mengchen Liu, Bin Xiao, Jianlong Fu, and Lu Yuan. Minivit: Compressing vision transformers with weight multiplexing. In *Proceedings of the IEEE/CVF Conference on Computer Vision and Pattern Recognition*, pp. 12145–12154, 2022a.
- Yuxin Zhang, Mingbao Lin, Zhihang Lin, Yiting Luo, Ke Li, Fei Chao, Yongjian Wu, and Rongrong Ji. Learning best combination for efficient n: M sparsity. In *Adv. Neural Inform. Process. Syst.*, pp. 941–953, 2022b.
- Zhun Zhong, Liang Zheng, Guoliang Kang, Shaozi Li, and Yi Yang. Random erasing data augmentation. In *Proceedings of the AAAI conference on artificial intelligence*, 2020.
- Mingjian Zhu, Kai Han, Yehui Tang, and Yunhe Wang. Visual transformer pruning. *arXiv e-prints*, pp. arXiv–2104, 2021.

A BOUND PROOF

In this section, we provide proof for the upper bound of pruning process:

$$\begin{aligned} & \sup_{\|x\|_2 \leq 1} \left\| f(x; W^{(1:L)}) - f(x; W^{(1:l-1)}, \widetilde{W}^{(l)}, W^{(l+1:L)}) \right\|_2 \\ & \leq \left\| W^{(l)} - \widetilde{W}^{(l)} \right\|_F \cdot \prod_{\substack{j \neq l \\ j \in [1, L]}} \left\| W^{(j)} \right\|_F \end{aligned} \quad (11)$$

Inspired by Neyshabur et al. (2015); Lee et al. (2020), we can write the network $f(x; W^{(1:L)})$ with its layers:

$$f(x; W^{(1:L)}) = W_L \sigma(W_{L-1} \sigma(W_{L-2} (\dots \sigma(W_1 x)))) \quad (12)$$

Then we can peel the highest layer W_L :

$$\begin{aligned} & \left\| f(x; W^{(1:L)}) - f(x; W^{(1:l-1)}, \widetilde{W}^{(l)}, W^{(l+1:L)}) \right\|_2 \\ & = \left\| W^{(l)} \left(\sigma(f(x; W^{(1:L-1)})) - \sigma(f(x; W^{(1:l-1)}, \widetilde{W}^{(l)}, W^{(l+1:L-1)})) \right) \right\|_2 \end{aligned} \quad (13)$$

With Cauchy-Schwarz inequality Steele (2004), we have the upper bound of Equation 13 as:

$$\left\| W^{(L)} \right\|_F \cdot \left\| \sigma(f(x; W^{(1:L-1)})) - \sigma(f(x; W^{(1:l-1)}, \widetilde{W}^{(l)}, W^{(l+1:L-1)})) \right\|_2 \quad (14)$$

Suppose σ is the ReLU activation, so we use the 1-Lipschitzness of ReLU activation with respect to ℓ_2 norm for the upper bound of Equation 14 as:

$$\left\| W^{(L)} \right\|_F \cdot \left\| f(x; W^{(1:L-1)}) - f(x; W^{(1:l-1)}, \widetilde{W}^{(l)}, W^{(l+1:L-1)}) \right\|_2 \quad (15)$$

Then we continue peeling the second highest layer W_{L-1} to lower layers and stop the peeling at the **pruned layer** $\widetilde{W}^{(l)}$. We have this upper bound for Equation 13:

$$\begin{aligned} & \left\| f(x; W^{(1:L)}) - f(x; W^{(1:l-1)}, \widetilde{W}^{(l)}, W^{(l+1:L)}) \right\|_2 \\ & \leq \left(\prod_{j>l} \left\| W^{(j)} \right\|_F \right) \cdot \left\| f(x; W^{(1:l)}) - f(x; W^{(1:l-1)}, \widetilde{W}^{(l)}) \right\|_2 \end{aligned} \quad (16)$$

We consider the effect of pruning for the term on the right side and use Cauchy-Schwarz inequality again:

$$\begin{aligned} \left\| f(x; W^{(1:l)}) - f(x; W^{(1:l-1)}, \widetilde{W}^{(l)}) \right\|_2 & = \left\| (W^{(l)} - \widetilde{W}^{(l)}) \sigma(f(x; W^{(1:l-1)})) \right\|_2 \\ & \leq \left\| W^{(l)} - \widetilde{W}^{(l)} \right\|_F \cdot \left\| \sigma(f(x; W^{(1:l-1)})) \right\|_2 \end{aligned} \quad (17)$$

For the activation term, based on $\sigma(\mathbf{0}) = \mathbf{0}$, we have:

$$\left\| \sigma(f(x; W^{(1:l-1)})) \right\|_2 = \left\| \sigma(f(x; W^{(1:l-1)})) - \sigma(\mathbf{0}) \right\|_2 \leq \left\| f(x; W^{(1:l-1)}) - \mathbf{0} \right\|_2 = \left\| f(x; W^{(1:l-1)}) \right\|_2. \quad (18)$$

If we continue the peeling process as shown in equation 13, we can achieve equation 11.

B MODULE DEFINITION

Attention-related Module (QKV-M and PRJ-M). Self-attention is an important operation in Swin Transformer. In every transformer block, there are two layers related to self-attention, that is, ATT-QKV and ATT-PRJ in Figure 3. ATT-QKV means the ‘‘Query, Key, and Value’’ matrix for self-attention, and ATT-PRJ indicates the projection layer for self-attention. Assuming \mathbf{z}^l is the feature map of l_{th} layer, two attention-related layers are:

$$\mathbf{z}^{l+1} = \text{ATT-QKV}(\mathbf{z}^l), \quad \mathbf{z}^{l+2} = \text{ATT-PRJ}(\mathbf{z}^{l+1}) \quad (19)$$

where \mathbf{z}^l is the input feature map of ATT-QKV, and \mathbf{z}^{l+1} is the input feature map of ATT-PRJ. After these two layers, there is a residual connection between the output of the ATT-PRJ layer and the feature map before the LN layer:

$$\hat{\mathbf{z}}^{l+2} = \mathbf{z}^{l+2} + \mathbf{z}^{l-1} \quad (20)$$

Assume there are J transformer blocks in the whole network. For the transformer block shown in Figure 3(a), assume the range of the layer index is $[l, l+5]$. For the j_{th} block after this block, the layer index range is $[l+p_j, l+p_j+5]$, where p_j means the number of layers between these two blocks. Then we can define QKV-M and PRJ-M as:

$$\begin{aligned} \text{QKV-M} &: \{\mathbf{W}^{l+1}, \dots, \mathbf{W}^{l+p_j+1}, \dots\} \quad \text{for } j \in [1, J]. \\ \text{PRJ-M} &: \{\mathbf{W}^{l+2}, \dots, \mathbf{W}^{l+p_j+2}, \dots\} \quad \text{for } j \in [1, J]. \end{aligned} \quad (21)$$

Multilayer Perceptron-related Module (MLP-M). Another important part of the Swin Transformer is the multilayer perceptron. There are two MLP layers in every Swin Transformer block. We name these two layers MLP-FC1 and MLP-FC2:

$$\mathbf{z}^{l+4} = \text{MLP-FC1}(\mathbf{z}^{l+3}), \quad \mathbf{z}^{l+5} = \text{MLP-FC2}(\mathbf{z}^{l+4}) \quad (22)$$

where \mathbf{z}^{l+3} is the input feature map of MLP-FC1, and \mathbf{z}^{l+4} is the input feature map of MLP-FC2. Similarly, after two MLP layers, there is a residual connection between the output of the MLP-FC2 layer and the feature map before the LN layer:

$$\hat{\mathbf{z}}^{l+5} = \mathbf{z}^{l+5} + \hat{\mathbf{z}}^{l+2} \quad (23)$$

Considering J blocks in the whole network, and $j \in [1, J]$, we can define the MLP-M as:

$$\text{MLP-M} : \{\mathbf{W}^{l+4}, \mathbf{W}^{l+5}, \dots, \mathbf{W}^{l+p_j+4}, \mathbf{W}^{l+p_j+5}, \dots\}. \quad (24)$$

Auxiliary Module (AUX-M). The auxiliary module consists of the auxiliary layers inside and outside the Swin Transformer block. Inside the Swin Transformer block, as shown in Figure 3(a), there are two LN layers. Some other auxiliary layers outside the Swin Transformer blocks, including a patch embedding layer and several patch merging layers, are also included in AUX-M. We do not prune these layers due to their important contribution to the network and their relatively small parameter count.